VERSITA

Cent. Eur. J. Chem. • 12(3) • 2014 • 312-317
DOI: 10.2478/s11532-013-0385-2

Central European Journal of **Chemistry**

Agglomeration of ZnS nanoparticles without capping additives at different temperatures

Short Communication

Petr Praus[1*], Richard Dvorský[2], Petr Kovář[3], Ladislav Svoboda[1]

[1]*Department of Analytical Chemistry and Material Testing, VŠB-Technical University of Ostrava, 708 33 Ostrava-Poruba, Czech Republic*

[2]*Institute of Physics, VŠB-Technical University of Ostrava, 708 33 Ostrava-Poruba, Czech Republic*

[3]*Department of Chemical Physics and Optics, Charles University in Prague, Faculty of Mathematics and Physics, 121 16 Prague 2, Czech Republic*

Received 12 May 2013; Accepted 12 November 2013

Abstract: ZnS nanoparticles were precipitated in diluted aqueous solutions of zinc and sulphide ions without capping additives at a temperature interval of 0.5–20°C. ZnS nanoparticles were arranged in large flocs that were disaggregated into smaller agglomerates with hydrodynamic sizes of 70–150 nm depending on temperature. A linear relationship between hydrodynamic radius (R_a) and temperature (T) was theoretically derived as $R_a = 652 - 2.11\,T$.

The radii of 1.9–2.2 nm of individual ZnS nanoparticles were calculated on the basis of gap energies estimated from their UV absorption spectra. Low zeta potentials of these dispersions of -5.0 mV to -6.3 mV did not depend on temperature. Interactions between individual ZnS nanoparticles were modelled in the Material Studio environment. Water molecules were found to stabilize ZnS nanoparticles *via* electrostatic interactions.

Keywords: *ZnS nanoparticles • Agglomeration • Low temperatures • Molecular modelling*

1. Introduction

In general, colloidal systems contain a large number of individual nanoparticles dispersed in some continuous medium moving by Brownian motion and colliding with one another so that i) they remain separated as individual nanoparticles or ii) form agglomerates by a processes called coagulation or flocculation [1]. Colloidal systems are mostly stabilized by various capping (surface coating) additives providing their steric and/or electrostatic stabilization or by deposition on solid supports [2-4].

Nanoparticles have many unique properties, such as high surface area to volume ratio, large surface area and energy *etc*. [5]. ZnS nanoparticles have some important properties typical for other semiconductor nanoparticles, including a quantum size effect [6], which predetermine them for luminescence and photocatalytic applications [7]. Synthesis, characterization and applications of semiconductor nanoparticles were reviewed in detail in, *e.g*. a book edited by Smith [2]. In particular, precipitation of ZnS nanoparticles in the presence of cationic surfactants was reviewed in our recent papers [8,9].

The aim of this study was to investigate the agglomeration of ZnS nanoparticles without capping additives at low temperatures reducing their kinetic energy of Brown's movement. These colloid dispersions were stabilized only by repulsive electrostatic interactions among ZnS nanoparticles. According to the von Weimarn law, colloidal dispersions can be obtained from very diluted or very concentrated solutions, therefore, ZnS nanoparticles were precipitated in diluted solutions of zinc and sulphide ions. Experimental techniques were

* *E-mail: petr. praus@vsb.cz*

completed by molecular modelling to understand interactions between individual nanoparticles in aqueous environments.

2. Experimental procedure

2.1. Material and chemicals

The chemicals used were of analytical reagent grade: zinc acetate and sodium sulphide (both from Lachema, Czech Republic). Water deionized by reverse osmosis (Aqua Osmotic, Czech Republic) was used for preparation of all solutions.

2.2. Precipitation of ZnS nanoparticles

In a typical procedure, 50 mL of the aqueous solution of Na_2S (2.5 mmol L^{-1}) was added drop-wise to 250 mL of aqueous solution of $Zn(CH_3COO)_2$ (0.3 mmol L^{-1}) under vigorous stirring and cooling. The molar ratio between zinc and sulphur precursors was kept at 1:1.7.

2.3. UV absorption spectra measurements

UV absorption spectra of ZnS colloidal dispersions were measured by a double-beam spectrometer Lambda 25 (Perkin Elmer, USA). All spectra were recorded using 1 cm quart cuvettes within a wavelength range from 200 nm to 400 nm.

2.4. Zeta potential and hydrodynamic size measurements

Zeta potentials and hydrodynamic sizes were measured by dynamic light scattering (DLS) at λ = 633 nm using a Zetasizer Nano ZS instrument (Malvern Instruments, UK). This instrument is able to measure particle sizes from 0.6 nm to 8.9 μm and zeta-potentials from -500 mV to + 500 mV. A sample of the ZnS dispersion was filtered through a membrane filter with a pore size < 100 nm and injected into the disposable capillary cell (DTS1061). The measurements of the zeta potentials and hydrodynamic sizes were performed immediately after precipitation using the SOP Player measurement programme sequence. In this manner, the fractions of nanoparticles with low zeta potentials could be registered before their flocculation.

2.5. Transmission electron microscopy

Transmission electron microscopy (TEM) was performed on a JEM 1230 (Jeol, Japan) microscope operated at 80 kV. Freshly prepared samples of ZnS nanoparticles were placed on a copper grid (400 mesh) coated by a Formvar film (1.5-3 wt.% of polyvinylformaldehyde in chloroform), dried by blotting paper and analyzed after 2 days. Contrast of micrographs was improved by a 1 wt.% solution of ammonium molybdate added to the samples.

2.6. Molecular simulations

Molecular modelling simulations were performed in the Forcite module of the Materials Studio modelling environment [10]. The wurtzite structure data were used for building ZnS nanoparticles. Crystallographic data for wurtzite are the following: space group P63mc, a = b = 0.382 nm, c = 0.626 nm [11]. The atomic positions were variable during geometry optimization. Molecular dynamics simulations were performed in an NVT statistical ensemble at a temperature of 298 K; one dynamics step was 0.5 ps and 500–1000 ps were performed. Atomic positions of ZnS nanoparticles were fixed during the simulations. After dynamics simulations the models were optimized with variable atomic positions.

ZnS nanoparticles were surrounded by 5860 water molecules. Charges of atoms in ZnS nanoparticles were calculated by the QEq method [12] and total charge for each ZnS nanoparticles was set to zero. Charges for water molecules were assigned by the Compass force field [13]. The models were optimized in the Universal force field [14]. Electrostatic and van der Waals interactions were calculated by a cubic spline with a cut-off distance of 1.55 nm.

3. Results and discussion

3.1. Agglomeration of ZnS nanoparticles

ZnS dispersions were examined by TEM, zeta potentials and hydrodynamic size measurements. TEM micrographs in Fig. 1 show large flocs of different sizes composed of individual ZnS nanoparticles, which seem to not create bulky particles but remain mutually separated. The flocs can be divided into smaller agglomerates indicated by circles.

Zeta potentials and hydrodynamic sizes (diameter), which depend on the temperature of ZnS dispersions, were measured using DLS as shown in Fig. 2. The zeta potentials within the temperature interval of 0.5–20°C were nearly constant, randomly changing between -5.0 mV and -6.0 mV. The low zeta potentials values were likely as a result of low amounts of adsorbed sulphide ions in the diluted solutions. In general, zeta potentials equal to or higher than *ca* ±30 mV are necessary to stabilize colloid dispersions. Therefore, the next experiments were performed immediately after precipitation to avoid coagulation at longer times. In

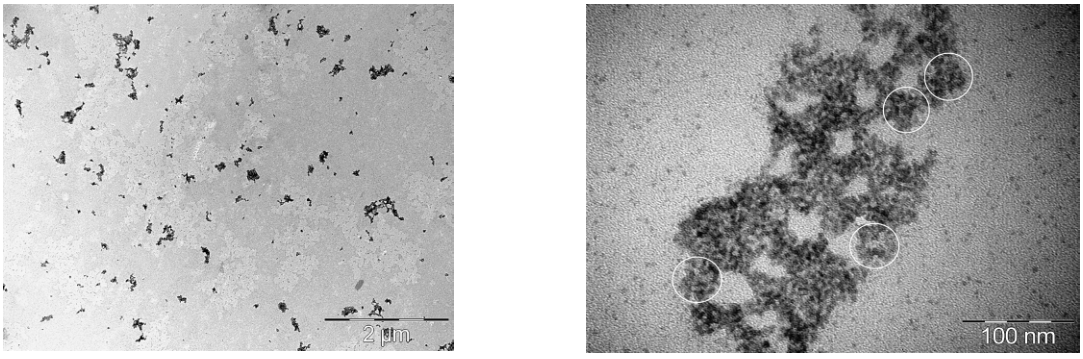

Figure 1. TEM micrographs of ZnS dispersions at 0.5°C. Overall view of ZnS flocs (left), detail view of one ZnS floc.

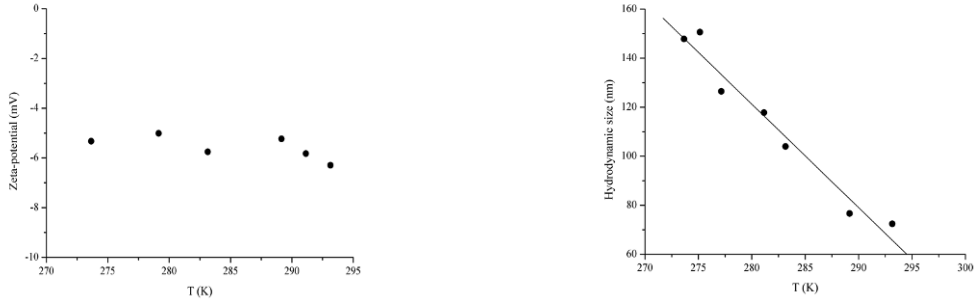

Figure 2. Zeta-potentials (left) and hydrodynamic sizes of ZnS colloidal dispersions as a function of thermodynamic temperature.

practice the experiments were performed at about 30 s after precipitation because our equipment was not able to analyse ZnS dispersions in very short time intervals after their precipitation like *e.g.* [15].

As mentioned above, we assumed that the large flocs depicted in Fig. 1 were composed of smaller agglomerates, which can be characterized by a mean radius R_a. Fig. 2 shows that the hydrodynamic size of ZnS agglomerates significantly decreased with increasing temperature. Hydrodynamic sizes were lognormaly distributed and only their mode values were evaluated. Each point in Fig. 2 was calculated as an average from 5–6 measurements; relative standard deviation varied from 4 to 20%. A mean mutual equilibrium distance h_0 between these agglomerates corresponds to the secondary shallow minimum on a potential function described by the DLVO theory [1]. According to this function the total interaction potential u (sum of attraction and repulsion potential) depends on a distance h between the agglomerates as follows

$$u(R_a) = \left[\frac{2\varepsilon\zeta}{l}\exp(-\frac{h}{l})\right] - \left[\frac{H}{12\pi h}\right]R_a \qquad (1)$$

where e is the permittivity, z is the zeta potential, l is the effective thickness of an electric bilayer of sulphide and zinc ions and H is the Hamaker constant. It is possible to emphasise here that both the flocs and smaller agglomerates were assumed to be composed of individual ZnS nanoparticles as demonstrated below. A stability of agglomerates of the radius R_a having the Brown kinetic energy of $\frac{3}{2}k_bT$ can be expressed as

$$\frac{3}{2}k_bT \le u(R_a) \qquad (2)$$

where the total potential $u(R_a)$ corresponds to the mean distance h_0 among them. For maximal R_a at temperature T we can obtain from Eqs. 1 and 2

$$\frac{3}{2}k_bT = \left[\frac{2\varepsilon\zeta}{l}\exp(-\frac{h_0}{l})\right] - \left[\frac{H}{12\pi h_0}\right]R_a \qquad (3)$$

Now we can derive a dependence of the agglomerate radius R_a on temperature as follows

$$R_a = \underbrace{\left[\frac{24\varepsilon\zeta\pi h_0}{Hl}\exp(-\frac{h_0}{l})\right]}_{\alpha} - \underbrace{\left[\frac{36k_b\pi h_0}{H}\right]}_{\beta}T \qquad (4)$$

where a and b are the constants; the parameter a can be considered constant because the zeta potentials z were found to be constant as demonstrated in Fig. 2. The decrease of the measured hydrodynamic radii R_a with increasing temperature can be well characterized by a linear relationship $R_a = 652 - 2.11\,T$ (with correlation coefficient r_c = 0.9807) in agreement with Eq. 4, which confirms the validity of our assumptions.

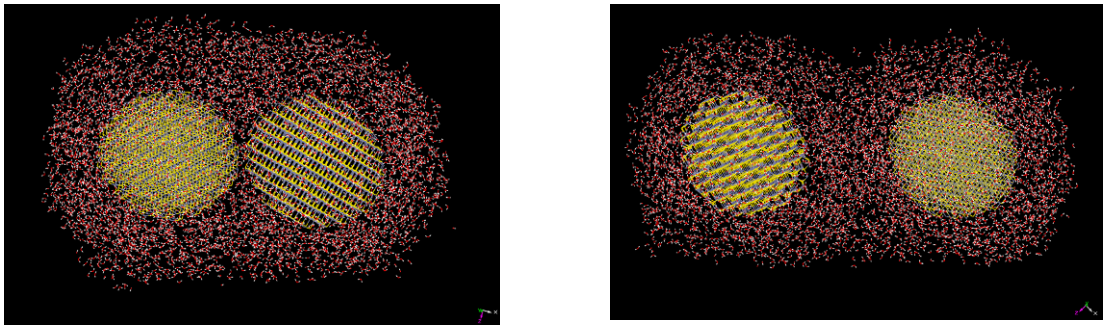

Figure 3. Simulations of two ZnS nanoparticles surrounded by water molecules in tight arrangement (left) and with mutual distance of 2.0 nm.

Table 1. Calculated sublimation energies for systems of ZnS nanoparticles and water.

System No.	E_{total} (kcal mol^{-1})	E_{elst} (kcal mol^{-1})	E_{vdw} (kcal mol^{-1})
1	-33475	-33217	-258
2	-36453	-36159	-294

3.2. Size of ZnS nanoparticles

The ZnS colloidal dispersions were studied by UV spectrometry supposing that the agglomerates were composed of individual nanoparticles exhibiting the quantum size effect [6]. The UV absorption spectra were recorded 30 s after precipitation within the temperature interval of 0.5–20°C to estimate gap energies of ZnS nanoparticles according to Tauc's method and consequently to calculate their radii similarly as in our earlier studies [8,9]. Bulk ZnS particles have a gap energy of about 3.7 eV, however, ZnS nanoparticles with sizes lower than 10 nm have larger gap energies as a result of the quantum size effect as

$$E_g(nano) = E_g(bulk) + \frac{h^2}{8r^2}\left(\frac{1}{m_e} + \frac{1}{m_h}\right) - \left(\frac{1.8e^2}{4\pi\varepsilon_r\varepsilon_0 r}\right) \quad (5)$$

where $E_g(nano)$ and $E_g(bulk)$ are the gap energies of ZnS nanoparticles and bulk particles, respectively, h is Planck's constant, r is the radius of nanoparticles, m_e and m_h are the effective masses of electron and hole, respectively, and ε_r is the relative permittivity dielectric constant of the material, ε_o is the permittivity of vacuum. For ZnS, $m_e = 0.42m_0$ and $m_h = 0.61m_0$, where m_0 is the free electron mass and $\varepsilon_r = 8.76$ [16].

The nanoparticles radii calculated according to Eq. 5 changed very little from 1.9 nm to 2.2 nm within the tested temperature interval. Such small radii confirmed our assumption that the agglomerates were composed of individual and mutually separated ZnS nanoparticles.

3.3. Molecular simulations of ZnS nanoparticles

Interactions between two ZnS nanoparticles surrounded by water molecules were simulated in the Forcite module of the Materials Studio modelling environment. The total charge of ZnS nanoparticles was set to zero, which was close to the determined low zeta potentials. The wurtzite ZnS structure [8] data were used for building the ZnS nanoparticles. According to the experimental data ZnS nanocrystals in the shape of a sphere with the radii of 2.0 nm were created and used for simulations. Two types of systems were created: i) system 1 with a tight arrangement of ZnS nanoparticles, where the distance between the centres of ZnS nanoparticles was 4.0 nm and ii) system 2 with ZnS nanoparticles isolated by water molecules where the mutual distance between the nanoparticle surfaces was about 2.0 nm and the distance between the nanoparticles centres was about 6.0 nm (Fig. 3).

Both systems were characterized by total sublimation energy E_{total} calculated as a sum of non-bonded energy - van der Waals (E_{vdw}) and electrostatic (E_{elst}) interactions ($E_{total} = E_{vdw} + E_{elst}$) between the rigid bodies in the systems. The rigid body is a part of a system, where all the interactions (bonded and non-bonded) between the atoms are not calculated. The total sublimation energy can give us information on stability, probability of existence and mutual interactions in the systems. In our case, rigid bodies were represented by water molecules and ZnS nanoparticles. The simulation results are summarized in Table 1.

Each non-bonded interaction E (E_{elst}, E_{vdw} and their sum E_{total}) was calculated as $E = E_{ZnS+H2O} - E_{H2O}$, where $E_{ZnS+H2O}$ is the interaction energy between all parts of the systems and E_{H2O} represents the interaction energy within a bulk of water surrounding ZnS nanoparticles. Total sublimation energy E_{total} involves the interactions between ZnS nanoparticles and water molecules and the interactions between ZnS nanoparticles themselves. One can see that electrostatic interactions are dominant in the E_{total} energy terms and the total energy of system

2 is about 8% lower than in system 1. This shows that system 2 of the isolated ZnS nanoparticles is more stable than system 1 with their tight arrangement.

Except ZnS and H_2O interactions it is useful to consider the interactions between ZnS nanoparticles. The interaction energies E_{total} between the ZnS nanoparticles were negative and for system 1 the value was of hundreds of kcal mol^{-1}. With increasing distance between ZnS nanoparticles the interaction energy increased. For example, at the distance of 1.2 nm the interaction energy was a hundred times lower (-2 kcal mol^{-1}) than for the system with their tight arrangement (-150 kcal mol^{-1}). This means that mutual interactions between ZnS nanoparticles can be influenced by their distance and the total sublimation energy of both systems is significantly influenced by water molecules.

If we consider the low concentration of ZnS nanoparticles in aqueous dispersions we can conclude that ZnS nanoparticles probably will be isolated by water molecules in their agglomerates. This agrees with the low ZnS radii of 1.9-2.2 nm estimated from the UV absorption spectra. In addition, the molecular simulations also indicated that water molecules can mediate electrostatic interactions stabilizing ZnS nanoparticles in their agglomerates.

4. Conclusions

ZnS nanoparticles were precipitated in diluted aqueous solutions of zinc and sulphide ions without any capping additives at temperatures of 0.5–20°C. ZnS dispersions consisted of flocks which were observed by TEM. With increasing temperature these flocs were broken down to smaller agglomerates with hydrodynamic sizes of 70–150 nm. The linear dependence between the hydrodynamic radius and thermodynamic temperature was theoretically derived and confirmed by experiments. The zeta potentials of these dispersions were constant at the temperature interval and reached the low values of -5 mV to -6.3 mV. The radii of 1.9–2.2 nm of individual ZnS nanoparticles were calculated on the basis of gap energies estimated from their UV absorption spectra.

In order to understand interactions between ZnS nanoparticles they were modelled in the Material Studio environment. The system with ZnS nanoparticles separated by water molecules was more stable than one with their tight arrangement. This indicates that water molecules intermediate stabilizing electrostatic interactions between the nanoparticles and it confirms the assumption that the nanoparticles were mutually separated in their agglomerates.

Both experimental and molecular simulations revealed that ZnS nanoparticles formed agglomerates but they existed as individual objects in their diluted dispersions. This study allowed us to investigate the behaviour of single ZnS nanoparticles without any capping additives like cationic surfactants. They are able to stabilize nanoparticles but strongly influence relationships among them during their growth and/or in agglomeration [8,9]. Next, experiments will be performed to investigate growth mechanisms of uncapped ZnS nanoparticles at different temperatures.

Acknowledgement

This work was supported by the Czech Science Foundation (P107/11/1918), by the Regional Materials Science and Technology Centre (CZ.1.05/2.1.00/01.0040) in Ostrava and by VŠB-Technical University of Ostrava (student's grant SP2013/56).

References

[1] R.J. Hunter, Foundations of Colloid Science, 2nd edition (Oxford University Press, Oxford, 2009) 1-43
[2] G. Smith (Ed.), Nanoparticles: From Theory to Applications, 2nd edition (Wiley-VCH, Weinheim, 2010)
[3] K.C. Kwiatkowski, Ch.M. Lukehart, In: H.S. Nalwa (Ed), Nanostructured Materials and Technology (Academic Press, London, 2002)
[4] B.R. Cuenya, Thin Solid Films 518(12), 3127 (2010)
[5] B. Tyagi, K.B. Sidhpuria, R.V. Jasra, In: H.S. Nalwa (Ed), Encyclopedia of Nanoscience and Nanotechnology (American Scientific Publishers, Valencia, USA, 2011) Vol. 17, 479-546
[6] L.E. Brus, J. Phys. Chem. 90(12) 2255 (1986)
[7] K. Rajeshwar, N.R.de Tacconi, C.R. Chenthamarakshan, Chem. Mater. 13(9), 2765 (2001)
[8] O. Kozák, P. Praus, K. Kočí, M. Klementová, J. Colloid Interf. Sci. 352(2), 244 (2010)
[9] P. Praus, R. Dvorský, P. Horínková, M. Pospíšil, P. Kovář, J. Colloid Interf. Sci. 377(1), 58 (2012)
[10] Materials Studio Modeling Environment, Release 4.3 Documentation (Accelrys Software Inc., San Diego, 2003)
[11] J.W. Anthony, R.A. Bideaux, K.W. Bladh, M.C. Nichols,(Eds.), Handbook of Mineralogy

(Mineralogical Society of America, Chantilly, 2013) http://www.handbookofmineralogy.org/ (accessed on 12th May 2013).
[12] A.K. Rappe, W.A. Goddard, J. Phys. Chem 95(8), 3358 (1991)
[13] H. Sun, D. Rigby, Spectrochim. Acta A 53(8), 1301 (1997)
[14] A.K. Rappe, C.J. Casewit, K.S. Colwell, W.A. Goddard, W.M. Skiff, J. Am. Chem. Soc. 114(25), 10024 (1992)
[15] M. Tieman, Ö. Weiß, J. Hartikainen, F. Marlow, M. Lindén, Chem. Phys. Chem. 6(10), 2113 (2005)
[16] K. Dutta, S. Manna, S.K. De, Synth. Met. 159(3-4), 315 (2009)